

Growth and Optical Properties of Wurtzite-Type CdS Nanocrystals

Huaqiang Cao,^{*,†} Guozhi Wang,[†] Sichun Zhang,[†] Xinrong Zhang,^{*,†} and Daniel Rabinovich[‡]

Department of Chemistry, Tsinghua University, Beijing 100084, People's Republic of China, and
Department of Chemistry, The University of North Carolina at Charlotte,
Charlotte, North Carolina 28223

Received March 15, 2006

This paper reports wurtzite-type CdS nanostructures synthesized via a hydrothermal reaction route using dithiol glycol as the sulfur source. The reaction time was found to play an important role in the shape of the CdS nanocrystals: from dots to wires via an oriented attachment mechanism. This work has enabled us to generate nanostructures with controllable geometric shapes and structures and thus optical properties. The CdS nanostructures show a hexagonal wurtzite phase confirmed by X-ray diffraction and show no evidence for a mixed phase of cubic symmetry. The Raman peak position of the characteristic first-order longitudinal optical phonon mode does not change greatly, and the corresponding full width at half-maximum is found to decrease with the CdS shape, changing from nanoparticles to nanowires because of crystalline quality improvement. The photoluminescence measurements indicate tunable optical properties just through a change in the shape of the CdS nanocrystals; i.e., CdS nanoparticles show a band-edge emission at ~ 426 nm in wavelength, while the CdS nanowires show a band-edge emission at ~ 426 nm as well as a weaker trap-state green emission at ~ 530 nm in wavelength. These samples provide an opportunity for the study of the evolution of crystal growth and optical properties, with the shape of the nanocrystals varying from nearly spherical particles to wires.

Introduction

Nanoscale semiconductors are of particular interest because of their unusual optoelectronic properties and potential applications, ranging from nanoscale electronic devices to light-emitting diodes,¹ biological labeling,² and so forth. Among these semiconductors, CdS, being one of the most important wide-gap semiconductors ($E_g \approx 2.5$ eV for the bulk hexagonal wurtzite phase of CdS and $E_g \approx 3.53$ eV for the "bulk" cubic zinc blende phase of CdS),³ has been extensively studied because of its ability to tune emission in the visible range simply by changing its size or shape.⁴

At present, it is one of the most important materials for nanoelectronics because it is possible to engineer the band gaps over a wide range from visible to ultraviolet.⁵ The utilization of nanomaterials inevitably requires sufficient control of their structures and their assembly systems because the intrinsic properties of the nanomaterials are determined by their structures, including size, shape, and dimension. Nanocrystalline CdS has been synthesized by a variety of

* To whom correspondence should be addressed. E-mail: hqcao@mail.tsinghua.edu.cn (H.C.), xrzhang@chem.tsinghua.edu.cn (X.Z.).

[†] Tsinghua University.

[‡] The University of North Carolina at Charlotte.

- (1) (a) Colvin, V. L.; Schlamp, M. C.; Alivisatos, A. P. *Nature* **1994**, *370*, 354. (b) Coe, S.; Woo, W. K.; Bawendi, M.; Bulovic, V. *Nature* **2002**, *420*, 800.
- (2) (a) Bruchez, M., Jr.; Moronne, M.; Gin, P.; Weiss, S.; Alivisatos, P. A. *Science* **1998**, *281*, 2013. (b) Chan, W. C. W.; Nie, S. M. *Science* **1998**, *281*, 2016. (c) Han, M.; Gao, X.; Su, J. Z.; Nie, S. *Nat. Biotechnol.* **2001**, *19*, 631. (d) Nirmal, M.; Brus, L. *Acc. Chem. Res.* **1999**, *32*, 407.
- (3) (a) Madelung, O.; Schulz, M.; Weiss, H., Eds. *Semiconductor Physics of Group II–VI Compounds*; New Series, Group III; Landolt-Börnstein: Berlin, 1982; Vol. 17, Part b. (b) Banerjee, R.; Jayakrishnan, R.; Ayyub, P. *J. Phys. Condens. Matter.* **2000**, *12*, 10647.

- (4) (a) Cao, H. Q.; Xu, Y.; Hong, J. M.; Liu, H. B.; Yin, G.; Li, B. L.; Tie, C. Y.; Xu, Z. *Adv. Mater.* **2001**, *13*, 1393. (b) Tang, K.; Qian, Y.; Zeng, J.; Yang, X. *Adv. Mater.* **2003**, *15*, 448. (c) Xiong, Y.; Xie, Y.; Yang, J.; Zhang, R.; Wu, C.; Du, G. *J. Mater. Chem.* **2002**, *12*, 3712. (d) Nedeljković, J. M.; Patel, R. C.; Kaufman, P.; Joyce-Pruden, C.; Leary, N. Ó. *J. Chem. Educ.* **1993**, *70*, 342. (e) Yang, C.; Awschalom, D. D.; Stucky, G. D. *Chem. Mater.* **2001**, *13*, 594. (f) Murakoshi, K.; Hosokawa, H.; Saitoh, M.; Wada, Y.; Sakata, T.; Mori, H.; Satoh, M.; Yanagida, S. *J. Chem. Soc., Faraday Trans.* **1998**, *94*, 579. (g) Lozada-Morales, R.; Zelaya-Angel, O.; Torres-Delgado, G. *Appl. Surf. Sci.* **2001**, *175–176*, 562. (h) Nagai, T.; Kanemitsu, Y.; Ando, M.; Kushida, T.; Nakamura, S.; Yamada, Y.; Taguchi, T. *Phys. Status Solidi B* **2002**, *229*, 611. (i) Kanemitsu, Y.; Ando, M.; Matsuda, K.; Saiki, T.; White, C. W. *Phys. Status Solidi A* **2002**, *190*, 537. (j) Shao, M.; Wu, Z.; Gao, F.; Ye, Y.; Wei, X. *J. Cryst. Growth* **2004**, *260*, 63. (k) Cao, Y. C.; Wang, J. *J. Am. Chem. Soc.* **2004**, *126*, 14336. (l) Pan, D.; Jiang, S.; An, L.; Jiang, B. *Adv. Mater.* **2004**, *16*, 982.
- (5) (a) Liu, S.-M.; Guo, H.-Q.; Zhang, Z.-H.; Li, R.; Chen, W.; Wang, Z.-G. *Phys. E (Amsterdam, Neth.)* **2000**, *8*, 174. (b) Bhattacharjee, B.; Ganguli, D.; Chaudhuri, S. *J. Fluoresc.* **2002**, *12*, 369.

methods including a sol–gel template,^{4a} a solvothermal route,^{4b} an in situ micelle–template-interface reaction route,^{4c} ion beam synthesis,⁴ⁱ ultrasonic irradiation in an aqueous solution,^{4j} one-pot synthesis,^{4k} a two-phase approach,^{4l} etc. The size, shape, and crystalline structure of semiconductor nanocrystallites are the important factors for determining their optical properties, which leads to considerable changes of the recombination of electrons and holes trapped at spatially separated donors and acceptors.

In this paper, we report a new route of controllable synthesis of wurtzite-type CdS nanoparticles and nanowires in bulk quantities. Organic molecule dithiol glycol (HSCH₂–CH₂SH) is used as the sulfur source.⁶ Through changes in the synthetic temperature and reaction time, CdS nanoparticle and nanowires can be controllably synthesized. The mechanism of self-assembly of CdS from nanoparticles to nanowires is discussed. The photoluminescence (PL) peaks change just because of the shape change of the CdS nanostructures.

Experimental Section

Synthesis. In a typical procedure, dithiol glycol (HSCH₂CH₂–SH; Eastgate, White lund, Morecambe, England, 98% purity) and Cd(NO₃)₂·4H₂O (analytical reagent, AR) were dissolved in 5 mL of alcohol (AR). In a typical case, 5 mL of a dithiol glycol (0.6 mmol) alcohol solution was added dropwise to 30 mL of a Cd(NO₃)₂ (1 mmol) aqueous solution at room temperature and stirred for 15 min. A mixture was obtained, then sealed in a 50-mL Teflon-lined autoclave, and maintained at 220–280 °C for 1–240 h. The light-yellow products were washed with deionized water and then in alcohol, and the cycle was repeated three times. The products were dried at 50 °C for 2 h.

Characterization. Products were characterized with X-ray diffraction (XRD; Bruker D8 advance), transmission electron microscopy (TEM; JEOL JEM-1200 transmission electron microscope operating at 120 kV), and Raman measurement (Renishaw RM 1000). Raman measurement was achieved using a microscopic confocal Raman spectrometer (Renishaw RM 1000) at room temperature. The 514-nm line of an Ar-ion laser with a power of about 5 mW was used to excite the Raman spectra. The diameter of the laser spot focused on the sample was ca. 1 μm. PL spectra were recorded with a fluorescence spectrophotometer (Jasco FP-6500). pH values were measured by an acidometer (PHSJ-3F).

Results and Discussion

Figure 1 shows XRD patterns recorded from the three typical samples synthesized at 220 °C for 1 h (denoted as CdS-1, Figure 1a), 120 h (denoted as CdS-120, Figure 1b), and 240 h (denoted as CdS-240, Figure 1c), respectively. The XRD patterns of all samples can be consistently indexed to the hexagonal wurtzite-type CdS, in which the several prominent peaks correspond to the reflection (100), (002), (101), (110), (103), (112), and (203) (JCPDS 41-1049). The distinctive reflection peaks at $2\theta = 28.4^\circ$ and 53° are evidence of a hexagonal CdS phase, while the absence of a reflection peak at $2\theta = 31.5^\circ$ is evidence of no incorporation of the cubic zinc blende phase CdS.⁷ Nevertheless, the

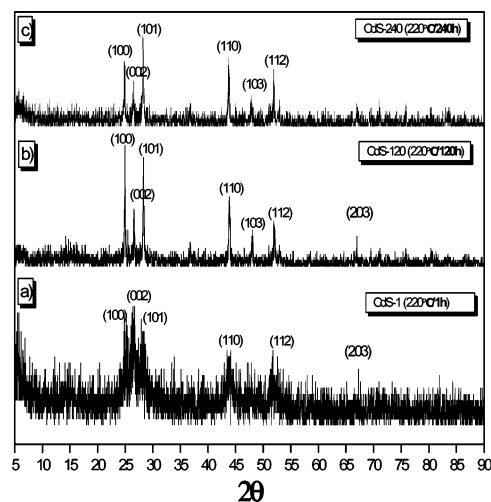


Figure 1. XRD patterns of samples synthesized at 220 °C for (a) 1 h (denoted as CdS-1), (b) 120 h (denoted as CdS-120), and (c) 240 h (denoted as CdS-240).

intensities of some diffraction lines were relatively enhanced with an increase in the reaction time from 1 to 240 h. The broadening of the diffraction peaks for CdS nanoparticles (CdS-1) is obvious, which indicates the formation of ultrafine particles. However, the relative intensities of the diffraction peaks of CdS nanowires (CdS-120 and CdS-240) deviate from those of CdS nanoparticles (CdS-1), suggesting a diffraction-oriented growth direction of the nanowire. The XRD patterns show a substantial texture effect in accordance with the crystal shape anisotropy and orientation. When the intensities of the (100), (002), and (101) peaks of CdS nanowires (CdS-120 and CdS-240) are compared with those of CdS nanoparticles (CdS-1), it is found that the relative maximum intensity sequence is no longer $(001) > (100) \approx (101)$ for CdS-1 but $(101) > (100) > (002)$ for CdS-240 and $(101) \approx (100) > (002)$ for CdS-120, implying that the nanowire growth occurs along the $\langle 101 \rangle$ direction. These changes can be attributed to the preferential orientation of the crystals. CdS is usually known to exist in two modifications: zinc blende and wurtzite-type phases.^{3b,8} The wurtzite-type structure is a uniaxial crystal with its optical axis parallel to the crystallographic axis *c*. In fact, wurtzite and zinc blende have similar lattice structures. Both of them own the same tetragonally positioned first nearest neighbors and nearly identical secondary nearest neighbors.⁹ Recently, it was also reported that a third phase, i.e., a high-pressure rock salt phase of CdS, was observed.¹⁰

It is well-known that vibrational spectroscopy is a very useful technique for the determination of the crystal phase. Furthermore, Raman spectroscopy of semiconductors is a

(6) Donahue, E. J.; Roxburgh, A.; Yurchenko, M. *Mater. Res. Bull.* **1998**, *33*, 323.

(7) Wang, W.; Germanenko, I.; Ei-Shall, M. S. *Chem. Mater.* **2002**, *14*, 3028.
 (8) (a) Lozada-Morales, R.; Zelaya-Angel, O.; Jiménez-Sandoval, S.; Torres-Delgado, G. *J. Raman Spectrosc.* **2002**, *33*, 460. (b) Filatova, E. O.; André, J.-M.; Taracheva, E. Yu.; Tvaladze, A. J.; Kraizman, V. L.; Novakovich, A. A.; Vedrinskii, R. V. *J. Phys. Condens. Matter.* **2004**, *16*, 4597.
 (9) Stampfl, A. P. J.; Hofmann, Ph.; Schaff, O.; Bradshaw, A. M. *Phys. Rev. B* **1997**, *55*, 9679.
 (10) Chen, C. C.; Herhold, A. B.; Johnson, C. S.; Alivisatos, A. P. *Science* **1997**, *276*, 398.

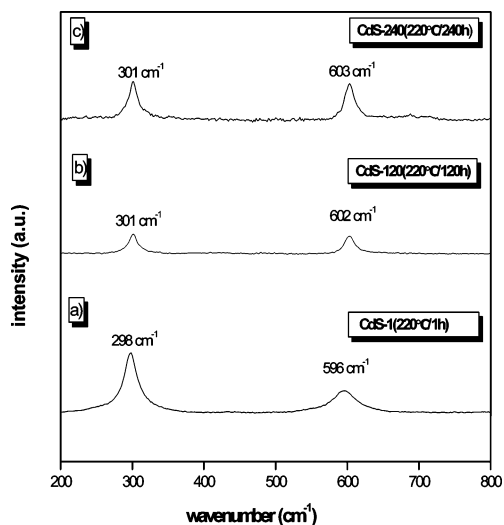


Figure 2. Raman spectra of samples synthesized at 220 °C for (a) 1 h (denoted as CdS-1), (b) 120 h (denoted as CdS-120), and (c) 240 h (denoted as CdS-240).

fast and nondestructive tool to appreciate crystalline material qualities, including surface conditions and homogeneity. That is, crystalline samples present sharp Raman peaks while amorphous or polycrystalline samples show very broad Raman peaks.¹¹ So, the structural characterization of the as-synthesized CdS nanostructures was therefore carried out using Raman spectroscopy. In Figure 2, Raman spectra of three typical samples, CdS-1, CdS-120, and CdS-240, are displayed. The Raman peaks of CdS-1 (nanoparticles) appear at 298 cm^{-1} , attributed to the $A_1(\text{LO})$ mode (where LO is a longitudinal optical phonon) with a full width at half-maximum (fwhm) of ca. 22.7 cm^{-1} and its overtone at 596 cm^{-1} . The Raman peaks of CdS-120 (nanowires attached with nanoparticles) appear at 301 cm^{-1} with a fwhm of ca. 14.7 cm^{-1} and its overtone at 602 cm^{-1} . The Raman peaks of CdS-240 (nanowires) appear at 301 cm^{-1} with a fwhm of ca. 15.2 cm^{-1} and its overtone at 603 cm^{-1} .^{6a,12} The Raman spectra exhibit relatively sharp crystal-like peaks. The decrease of the fwhm from nanoparticles (CdS-1) to nanowires (CdS-120 and CdS-240) can be attributed to the improvement of the crystallinity of the CdS nanocrystals. It has been reported that defect-free crystalline CdS films have a fwhm of 8 cm^{-1} .¹³ Also, this phenomenon has been demonstrated by the corresponding electron diffraction (ED) in TEM measurement, which is a single-crystalline structure for CdS nanowires (the insets in Figure 3d,e,i). We all know that in a crystalline semiconductor or insulator the observed Raman shifts usually correspond to the LOs, whereas other modes such as the transverse optical and surface phonon modes are not observable because of symmetry restrictions and their low intensities.¹⁴ Another observation is that the peak profile is almost symmetric for all three samples. It is

also observed that the intensity of the Raman line of sample CdS-120 is lower than that of CdS-1, which is attributed to the quantity of the sample detected by Raman. It is known that the intensity of a Raman line is proportional to the number of scattering centers because of the fact that Raman scattering is an incoherent process.¹⁵

Assembly of a nanocomponent is a key step for the construction of nanodevices; thus, the shape of the nanobuilding blocks will be crucial for the assembly and device design. Shape-controlled synthesis of the nanobuilding blocks is still a technique challenge for us. Generally, it is believed that Ostwald ripening¹⁶ is the main manner for crystal growth. Recently, a new oriented attachment mechanism is found under hydrothermal¹⁷ and refluxing solution conditions¹⁸ to form high-quality oxide nanorods or nanowires from nanoparticles, such as TiO_2 ,^{16a} MnO_3 ,^{17b} and ZnO .^{17c,18} Weller et al. suggested that oxide nanoparticles are very favorable for oriented attachment.¹⁸ Obviously, the essential requirement for wirelike structure formation is anisotropic crystal growth, which can usually be realized when the free surface energies of the various crystallographic planes differ obviously. We carried out several experiments in different ways to probe into the growth mechanism of as-synthesized CdS nanostructures. All of the experiments described hereafter were performed under hydrothermal conditions. Details can be found in the Experimental Section. Parts a–c of Figure 3 display CdS nanoparticles synthesized at 220 °C for 1 h (denoted as CdS-1), 2 h (denoted as CdS-2), and 3 h (denoted as CdS-3) with average particle sizes of approximately ~ 9.6 , ~ 17.2 , and ~ 17.9 nm, respectively. The corresponding powder XRD of CdS-1 is depicted in Figure 1 (curve a). It exhibits the typical size-broadened reflection from wurtzite-type CdS. The estimation of the primary crystallite size of this sample was ~ 7.3 nm, obtained by Scherrer line-width analysis of the reflection peaks. This result is consistent with the TEM observation. When the reaction time is increased to 4 h at 220 °C (denoted as CdS-4), we find that most of CdS are in the form of nanowires attached with some nanoparticles (Figure 3d). If the reaction time is increased to 24, 36, 48, and 120 h (denoted as CdS-24, CdS-36, CdS-48, and CdS-120, respectively) at 220 °C, we also obtain nanowires attached with some particles (Figure 3e–h). The corresponding XRD pattern of CdS-120 is presented in Figure 1 (curve b), which indicates that it belongs to

(11) Nandakumar, P.; Vijayan, C.; Rajakshmi, M.; Arora, A. K.; Murti, Y. V. G. S. *Phys. E (Amsterdam, Neth.)* **2001**, *11*, 377.
 (12) (a) Arguello, C. A.; Rousseau, D. L.; Porto, S. P. S. *Phys. Rev.* **1969**, *181*, 1351. (b) Abdulkhadar, M.; Thomas, B. *Nanostruct. Mater.* **1995**, *5*, 289.
 (13) Froment, M.; Bernard, M. C.; Cortes, R.; Mokili, B.; Lincot, D. *J. Electrochem. Soc.* **1995**, *142*, 2642.

(14) Nanda, K. K.; Sarangi, S. N.; Sahu, S. N.; Deb, S. K.; Behera, S. N. *Phys. B* **1999**, *262*, 31.
 (15) (a) Brunner, H.; Sussner, H. *Biochim. Biophys. Acta* **1972**, *271*, 16. (b) Xu, Y. M., Ed. *Raman Spectra and Its Applications in Structural Biology*; Chemical Industry Press: Beijing, China, 2005; p 7. (c) Huang, H. Z., Ed. *Nanomaterials Analysis*; Chemical Industry Press: Beijing, China, 2003; p 327.
 (16) (a) Banfield, J. F.; Welch, S. A.; Zhang, H.; Ebert, T. T.; Penn, R. L. *Science* **2000**, *289*, 751. (b) Murray, C. B.; Norris, D. J.; Bawendi, M. G. *J. Am. Chem. Soc.* **1993**, *115*, 8706. (c) Routkevitch, D.; Haslett, T. L.; Ryan, L.; Bigioni, T.; Douketis, C.; Moskovits, M. *Chem. Phys.* **1996**, *210*, 343.
 (17) (a) Penn, R. L.; Banfield, J. F. *Science* **1998**, *281*, 969. (b) Lou, X. W.; Zeng, H. C. *J. Am. Chem. Soc.* **2003**, *125*, 2697. (c) Liu, B.; Zeng, H. C. *J. Am. Chem. Soc.* **2003**, *125*, 4430.
 (18) Pacholski, C.; Kornowski, A.; Weller, H. *Angew. Chem., Int. Ed.* **2002**, *41*, 1188.

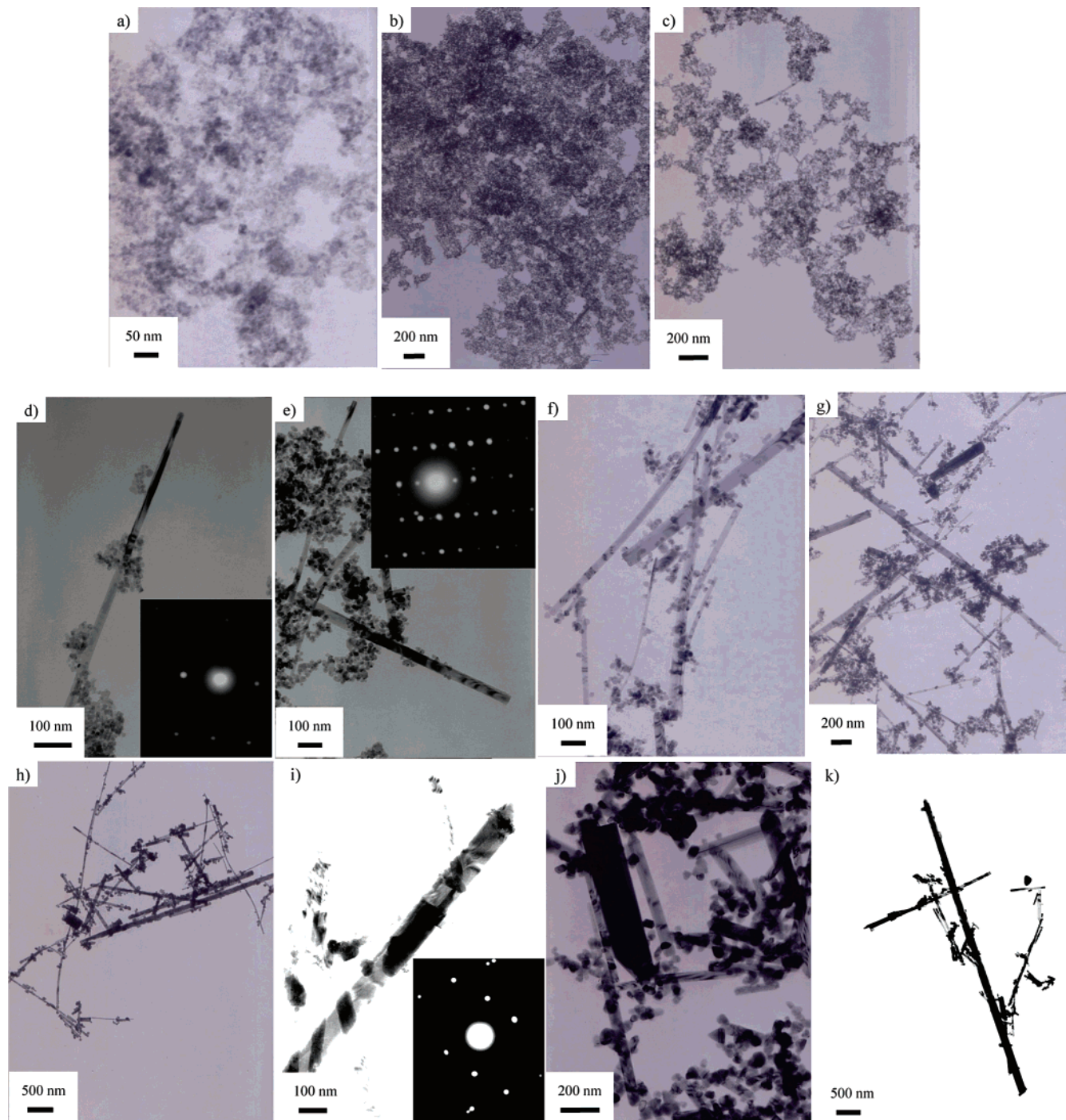


Figure 3. TEM images of as-synthesized samples at different conditions with the same concentration (a–j) for (a) at 220 °C for 1 h, (b) at 220 °C for 2 h, (c) at 220 °C for 3 h, (d) at 220 °C for 4 h, with the inset corresponding to ED, (e) at 220 °C for 24 h, with the inset corresponding to ED, (f) at 220 °C for 36 h, (g) at 220 °C for 48 h, (h) at 220 °C for 120 h, (i) at 220 °C for 240 h, with the inset corresponding to ED, (j) at 280 °C for 240 h, and (k) at 220 °C for 240 h, with the concentration being raised three times compared with all samples mentioned above including samples a–j.

hexagonal CdS. We find an interesting phenomenon; that is, all of these samples are present in the form of nanowires attached by some particles, and the longer the reaction time, the fewer the number of particles that are attached to the nanowires. Also, the wires belong to a single-crystalline structure, as is demonstrated by the corresponding ED pattern in TEM images (insets in Figure 3d,e). When the reaction time reaches 240 h at 220 °C (denoted as CdS-240, Figure 3i), we can obtain single-crystal nanowires only, corresponding the XRD presented in Figure 1 (curve c). Also, under

this condition, we can obtain nanowires with maximum length reaching $\sim 2.3 \mu\text{m}$, diameter $\sim 71 \text{ nm}$, and aspect ratio ~ 33 . If we raise the reaction temperature to 280 °C for 24 h (denoted as CdS-280-24), we can obtain wider CdS nanowires (Figure 3j) with maximum length $\sim 0.6 \mu\text{m}$, diameter $\sim 56 \text{ nm}$, and aspect ratio ~ 11 . If we raise the concentration of the initial reactants three times compared with all of the above-mentioned samples and keep the reaction temperature at 220 °C for 240 h, we can obtain longer and wider CdS nanowires with maximum length ~ 6.5

Growth and PL of Hexagonal CdS Nanocrystals

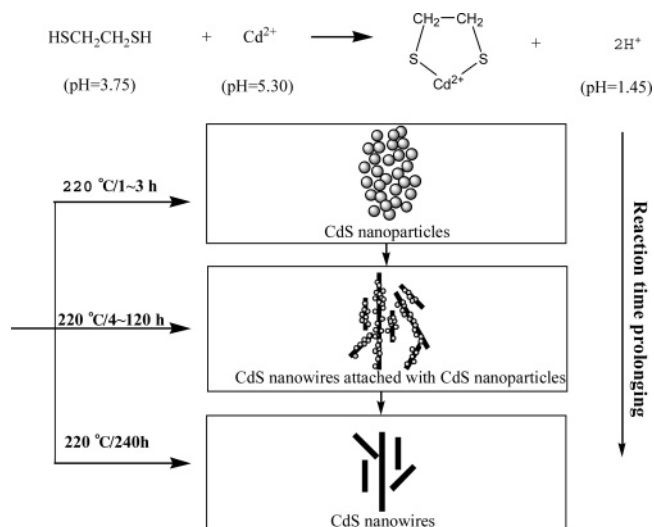


Figure 4. Strategy for the preparation of CdS nanoparticles and nanowires and the nanowire generated from nanoparticles via an oriented attachment mechanism.

μm , diameter ~ 158 nm, and aspect ratio ~ 42 (Figure 3k). However, if we reduce the reaction temperature to 190 °C for 4 or 24 h, we do not obtain CdS nanowires.

We believe that, before the hydrothermal reaction, the coordination occurs between $\text{HSCH}_2\text{CH}_2\text{SH}$ and Cd^{2+} and forms stable five-membered-ring coordination cation, which is demonstrated by a change of the pH value. After a $\text{HSCH}_2\text{CH}_2\text{SH}$ -alcohol solution (pH = 3.75) is added dropwise to a $\text{Cd}(\text{NO}_3)_2$ aqueous solution (pH = 5.30) with stirring for 15 min, the pH value of the resulting mixture is 1.45. This phenomenon is attributed to the coordination reaction between $\text{HSCH}_2\text{CH}_2\text{SH}$ and Cd^{2+} (Figure 4). After the hydrothermal reaction, the C-S bond in five-membered-ring coordination Cd^{2+} is broken and forms CdS. The coordination between -SH and Cd^{2+} may compete with the CdS crystal growth. If the reaction time is short, such as 1-3 h, we obtain CdS nanoparticles (Figure 3a-c). It has been demonstrated that crystalline structures of nanoparticles depend on their surface conditions because of their large surface-to-volume ratios.^{4f,19} So, the strong solvation of the solvent molecules $\text{HSCH}_2\text{CH}_2\text{SH}$ to Cd^{2+} and the surface Cd atoms of CdS nanoparticles leads to the generation of hexagonal CdS nanoparticles. After prolonging the hydrothermal reaction time, all of the C-S bonds are broken. Also, these CdS particles assembled under hydrothermal conditions via an “oriented attachment” mechanism,^{17,18} i.e., spontaneous self-organization of adjacent particles so that these nanoparticles share a common crystallographic orientation, followed by the joining of these particles at a planar interface.^{17a} The results of the experiment for changing the reaction time provide a strong evidence of the evolution process from the nanoparticles to nanowires (Figure 3). The increase of the reaction time mainly leads to an increase of the elongations of the CdS particles. According to the present experiment results, we can obtain clear evidence that oriented attachment

(19) (a) Tolbert, S. H.; Alivisatos, A. P. *Science* **1994**, *265*, 373. (b) Brus, L. E.; Harkless, J. A. W.; Stillinger, F. H. *J. Am. Chem. Soc.* **1996**, *118*, 4834.

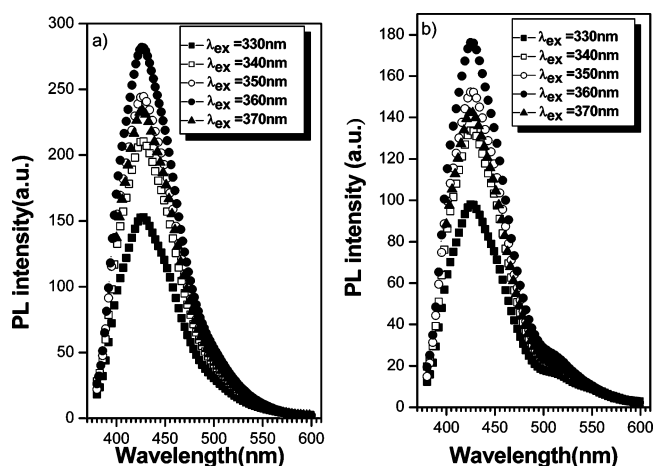


Figure 5. PL spectra of typical samples dispersed in ethanol: (a) CdS-1; (b) CdS-240.

of preformed quasi-spherical CdS nanoparticles is a major reaction path during the generation of single-crystalline hexagonal CdS nanowires under hydrothermal conditions. Our results may further demonstrate that the wurtzite structure itself favors oriented attachment no matter whether it is an oxide¹⁸ or sulfide.

The PL emissions from CdS nanoparticles (CdS-1) are shown in Figure 5a. All spectra exhibit the same emission maximum at 426 nm in wavelength violet light (2.91 eV in photon energy) and a similar peak shape with excitation wavelength ranging from 330 to 370 nm. Earlier reports indicate that CdS nanodots exhibit a band-edge PL emission peak centered at ~ 2.8 eV in photon energy (~ 443 nm in wavelength)^{8b} and surface-capped CdS nanocrystals exhibit a band-edge PL emission peak centered at ~ 2.6 eV (476 nm in wavelength).²⁰ Interestingly, emission at higher wavelengths (or lower energies), which has been attributed to deep trap states due to the surface,²¹ is not observed in our CdS nanoparticles, indicating that they are high-quality-size monodisperse CdS nanocrystals. In contrast, Figure 5b displays PL emission peaks from CdS nanowires (CdS-240) around ~ 530 nm as well as ~ 426 nm excited with $\lambda_{\text{ex}} = 330-370$ nm. The emission spectra are almost independent of the excitation wavelength used ($\lambda_{\text{ex}} = 330-370$ nm), with the maximum PL intensity present at $\lambda_{\text{ex}} = 360$ nm. The results indicate that the PL emission comes from the CdS nanocrystals, not from other impurities, which is due to band-edge emission and radiative recombination of e^-h^+ pairs at surface sulfur vacancy.²² We all know that CdS is an n-type semiconductor.^{3b,23} The smaller the ion radius is, the easier it is to yield vacancies.²³ So, it is easier to yield V_{S}

(20) (a) Okamoto, S.; Kanemitsu, Y.; Hosokawa, H.; Murakoshi, K.; Yanagida, S. *Solid State Commun.* **1998**, *105*, 7. (b) Joo, J.; Na, H. B.; Yu, T.; Yu, J. H.; Kim, Y. W.; Wu, F.; Zhang, J. Z.; Hyeon, T. *J. Am. Chem. Soc.* **2003**, *125*, 11100.

(21) (a) Murray, C. B.; Norris, D.; Bawendi, M. G. *J. Am. Chem. Soc.* **1993**, *115*, 8706. (b) Wang, Y.; Suna, A.; McHugh, J.; Hilinski, E. F.; Lucas, P. A.; Johnson, R. D. *J. Chem. Phys.* **1990**, *92*, 6927. (c) Bawendi, M. G.; Carroll, P. J.; Wilson, W. L.; Brus, L. E. *J. Chem. Phys.* **1992**, *96*, 946.

(22) (a) Ramsden, J. J.; Grätzel, M. *J. Chem. Soc., Faraday Trans.* **1984**, *80*, 919. (b) Brus, L. *J. Phys. Chem.* **1986**, *90*, 2555. (c) Murakoshi, K.; Hosokawa, H.; Saitoh, M.; Wada, Y.; Sakata, T.; Mori, H.; Satoh, M.; Yanagida, S. *J. Chem. Soc., Faraday Trans.* **1998**, *94*, 579.

because of $r(\text{S}^{2-}) < r(\text{Cd}^{2+})$. That means it will ionize electrons upon optical excitation, i.e.



V_S is a neutral sulfur vacancy, V_S^{**} is a doubly ionized sulfur vacancy, and e' is an electron in the conduction band, according to Kröger's notation.^{23,24} The PL spectra of the CdS nanowires show a predominant band-edge emission at ~ 426 nm and a weaker trap-state green-light emission at ~ 530 nm in wavelength, indicating a number of trap states, whose surface-to-volume ratio is higher than that in CdS nanoparticles, and this increases the occurrence of the surface trap states. A similar trap-state emission at 540 nm is also observed for CdS nanocrystals.^{2b,22} In fact, recent reports by Alivisatos and co-workers demonstrate that CdSe nanocrystals own polarized emission along the long axis, unlike spherical dots.^{25,25} This indicates that the ability to control the shapes of the semiconductor nanocrystals provides an opportunity to prepare materials with desirable optical characteristics from the point of view of application.

(23) Yang, S.; Wang, Z.; Wang, J., Eds. *Semiconductor Materials*; Science Press: Beijing, China, 2004.

(24) Kröger, F. A. *Chemistry of Imperfect Crystals*; North-Holland: Amsterdam, The Netherlands, 1964.

(25) (a) Peng, X.; Manna, L.; Yang, W.; Wickham, J.; Scher, E.; Kadavanich, A.; Alivisatos, A. P. *Nature* **2000**, *404*, 59. (b) Hu, J.; Li, L.; Yang, W.; Manna, L.; Wang, L.; Alivisatos, A. P. *Science* **2001**, *292*, 2060. (c) Li, L.; Hu, J.; Yang, W.; Alivisatos, A. P. *Nano Lett.* **2001**, *1*, 349.

Conclusion

To summarize, we have synthesized hexagonal CdS nanowires and nanoparticles as low as 220 °C. This provides a strong evidence of II–VI semiconductor nanocrystals besides the fact that oxide particles also are favorable via oriented attachment to construct nanowires, which offers an excellent method to design and synthesize anisotropic materials and properties. These phenomena can also help to understand the particle growth mechanism under hydrothermal conditions and to provide comparable materials with different morphologies (such as nanowires and nanoparticles synthesized in the same reaction systems) and properties. The PL properties of the CdS nanocrystals were investigated at room temperature. A violet-light band-edge emission at 426 nm from CdS nanoparticles and a green-light emission at 530 nm due to trap-state as well as band-edge emission at 426 nm from CdS nanowires were detected under optical excitation. This demonstrates that the nanometer-sized inorganic particles and wires exhibit a wide range of electrical and optical properties that is sensitive to both shape and size.²⁴

Acknowledgment. This work was supported by the Program for New Century Excellent Talents in University of the Education Ministry (Grant NCET-04-0066), the Foundation for the Author of National Excellent Doctoral Dissertation of P. R. China (Grant 200321), and the National Natural Science Foundation of China (Grants 20375002 and 20345005). Prof. D. Rabinovich also acknowledges support from The University of North Carolina at Charlotte.

IC060440C